2526

Combination of EGFR and MEK1/2 inhibitor shows synergistic effects by suppressing EGFR/HER3-dependent AKT activation in human gastric cancer cells

Young-Kwang Yoon,[1] Hwang-Phill Kim,[1]
Sae-Won Han,[2] Hyung-Seok Hur,[1] Do Youn Oh,[1,2]
Seock-Ah Im,[1,2] Yung-Jue Bang,[1,2,3]
and Tae-You Kim[1,2,3]

[1]Cancer Research Institute, [2]Department of Internal Medicine,
College of Medicine, and [3]Department of Molecular Medicine and
Biopharmaceutical Science, Graduate School of Convergence
Science and Technology, Seoul National University, Seoul, Korea

Abstract

EGFR tyrosine kinase inhibitors have shown promising efficacy in the treatment of tumors with *EGFR* mutations and amplifications. However, tyrosine kinase inhibitors have also proven ineffective against most tumors with *EGFR* wild-type (WT) alleles. Although some genetic changes, including the *KRAS* mutation, have been shown to confer resistance to tyrosine kinase inhibitors, novel strategies for the treatment of cancer patients with tumors harboring *EGFR* WT alleles have yet to be thoroughly delineated. The principal objective of this study was to improve our current understanding of drug interactions between EGFR and MAP/ERK kinase (MEK) inhibitors in an effort to gain insight into a novel therapeutic strategy against *EGFR* WT tumors. Using a panel of human *EGFR* WT gastric cancer cell lines, we showed that gastric cancer cells harboring the *KRAS* mutation were selectively sensitive to MEK inhibition as compared with those cells harboring *KRAS* and *PI3K* mutations and *KRAS* WT alleles. However, all cell lines were found to be resistant to EGFR inhibition. The results from Western blots and phosphoprotein arrays showed that, in MEK inhibitor resistant cell lines, AKT was activated through the EGFR/HER3/PI3K pathway following AZD6244 (ARRY-142886) treatment. Blockade of this feedback mechanism through the targeting of MEK and EGFR resulted in detectable synergistic effects in some cell lines *in vitro* and *in vivo*. Our results provide the basis for a rational combination strategy against human *EGFR* WT gastric cancers, predicated on the understanding of cross-talk between the MEK and EGFR pathways. [Mol Cancer Ther 2009;8(9):2526–36]

Introduction

The current broad use of anticancer agents will eventually lead to more personalized cancer therapeutic modalities, and the particular molecular profiles of the patient's tumor will ultimately guide the therapeutic choices made (1). These expectations are clearly linked to the development of selected kinase inhibitors in clinical settings (2). There is now compelling evidence to suggest that the activation of mutations in signaling pathways may result in "addiction" to these pathways, and thus, these mutations can be considered biomarkers to predict clinical responses to the inhibition of these pathways (3). This concept of context-dependent oncogene addiction has critical implications with regard to the identification of potential molecular biomarkers, as well as the design of molecular-targeted therapies (4, 5).

The overexpression of epidermal growth factor receptor (EGFR) and its ligands have been detected and reported in a variety of tumor types, and these findings have generated interest in EGFR as a potential target for cancer therapies (6). The identification of activating *EGFR* mutations in lung tumors that respond to EGFR tyrosine kinase inhibitors provides clinical proof of the concept of "oncogene addiction" (7–10). However, some lung cancer patients whose tumors harbor activating *EGFR* mutations have been shown to become refractory to tyrosine kinase inhibitors (11, 12), and thus, this strategy for EGFR dependency targeting currently is restricted to a small number of patients (7).

In patients with *EGFR* wild-type (WT) alleles, the resistance mechanisms of tyrosine kinase inhibitors may be induced by other genetic alterations, including *PI3K*, *BRAF*, or *KRAS* mutation, *PTEN* loss, and *MET* amplification (13–16). Among these, activating mutations of *KRAS* have been noted frequently in several tumor types (17, 18); interestingly, *EGFR* and *KRAS* mutations are rarely detected in the same tumors. This suggests that they may do functionally equivalent roles in tumors (19, 20). Considering these factors, *KRAS* mutations are related strongly with the prediction of primary sensitivity or resistance to tyrosine kinase inhibitors, as well as EGFR monoclonal antibody (15, 21).

The results of a recent high-throughput oncogene mutation profiling study have shown that oncogene mutations occur not only in a mutually exclusive fashion, like the *EGFR* and *KRAS* mutations, but also co-occur, such as in the case of *PIK3CA* and *KRAS* in human cancers (20). Moreover, the results of this study showed that rare and potentially "druggable" oncogenic mutations may exist in many common tumor types regarded as WT against well-known oncogenes (20). Thus, there is a clear need for more rational therapeutic strategies of genetically complex tumor cells, and several studies have already provided initial rational combination therapies (22–24). In this study, we characterize AZD6244 (ARRY-142886), a novel MAP/ERK kinase (MEK) inhibitor that exerts antiproliferative effects on human gastric cancer cell lines that are resistant to gefitinib. Furthermore, we suggest that the dual inhibition of EGFR and MEK1/2 signaling pathways may constitute a potent therapeutic strategy for the treatment of subsets of human *EGFR* WT gastric cancers.

Materials and Methods

Mutational Analysis of *EGFR*, *KRAS*, and *BRAF* Gene

Genomic DNA was extracted from nine gastric cancer cell lines. *EGFR* (exons 18–24), *KRAS* (exons 1–3), and *BRAF* (exon 15) were then sequenced using the previously described primers and methods (10, 25, 26). All sequencing reactions were conducted in the forward and reverse directions. All mutations were confirmed at least twice from independent PCR isolates, as described previously (10, 25).

Cell Culture and Reagents

Human gastric cancer cell lines (SNU-1, 5, 16, 484, 601, 638, 668, and 719) were obtained from the Korea Cell Line Bank (27), and AGS was purchased from the American Type Culture Collection. These cell lines were grown at 37°C under 5% CO_2 in RPMI-1640 containing 10% fetal bovine serum (WELGENE, Inc.). Gefitinib and AZD6244 were generously provided by AstraZeneca. SU11274 and LY294002 were purchased from Calbiochem. Stock solutions (10 μmol/L) were prepared in DMSO and stored at −20°C. Gefitinib, AZD6244, and SU11274 were diluted in fresh media before each experiment, and the final concentration of DMSO was <0.1%.

Antibodies and Western Blotting

Cultured cells were washed in ice-cold PBS and lysed in radioimmunoprecipitation assay buffer in accordance with the previously described methods (28). Samples containing equal quantities of total proteins were resolved on SDS-polyacrylamide denaturing gel, transferred to nitrocellulose membranes, and probed with antibodies. Detection was conducted using an enhanced chemiluminescence system (Amersham Pharmacia Biotech). Antibodies against p-EGFR (pY-1068), p-HER2 (pY-1221/1222), p-HER3 (pY-1289), p-MET (pY-1234/1235), p-PTEN (pS-380), p-STAT3 (pY-705), p-AKT (pS-473), p-ERK (pThr-202/Tyr-204), EGFR, HER2, MET, PTEN, STAT3, AKT, ERK, cyclin D, Bcl-2 interacting mediator of cell death (Bim), Bcl-xL/Bcl-2-associated death promoter (Bad), Myeloid Cell Leukemia-1 (MCL-1),

Bcl, Bcl-Xl, and caspase-3 were purchased from Cell Signaling Technology. Anti-HER3 antibody was acquired from Millipore. Bax, poly(ADP-ribose) polymerase, cyclin E, cyclin A, cyclin B, β-actin, p27, and p21 antibodies were obtained from Santa Cruz Biotechnology. Antitubulin antibody was purchased from Sigma-Aldrich.

Phospho–Receptor Tyrosine Kinase (RTK) and Phospho–Mitogen Activated Protein Kinase (MAPK) Arrays

Phospho-RTK and -MAPK arrays were purchased from R&D Systems and were conducted in accordance with the manufacturer's instructions.

Cell Growth Inhibition Assay

Tetrazolium dye (MTT; Sigma-Aldrich) assays were used to evaluate the growth inhibitory effects of AZD6244, gefitinib, or AZD6244 plus gefitinib. The cells were seeded on 96-well plates at a density of 3,000 cells per well, incubated for 24 h, and then treated for 72 h with drugs at 37°C. After drug treatment, MTT solution was added to each well and incubated for 4 h at 37°C before the removal of the media. DMSO was then added and mixed thoroughly for 30 min at room temperature. Cell viability was determined by measuring absorbance at 540 nm in a microplate reader (VersaMax, Molecular Devices). The drug concentrations required to inhibit cell growth by 50% were determined through interpolation from the dose-response curves (Calcusyn, Biosoft). Six replicate wells were used for each analysis, and at least three independent experiments were conducted. The data from replicate wells are presented as the mean numbers of remaining cells, with 95% confidence intervals. To determine the effects of the combined drug treatments, any potentiation was estimated by multiplying the percentage of remaining cells (percent growth) for each drug. The classification indices were calculated as previously described (29). Synergism was defined as % $AB/(\% A \times \% B) > 1.0$; additivity was defined as % $AB/(\% A \times \% B) = 0.9$ to 1.0; and antagonism was defined as % $AB/(\% A \times \% B) < 0.9$ (in these equations, A and B are the effects of individual agents, and AB represents the effects of the combination of the two drugs).

Cell Cycle Analysis and Annexin V Staining

Cells were treated for 24 h with drugs, washed twice in PBS, fixed in 70% ethanol, and then stored at −20°C until analysis. Before analysis, the cell suspensions were washed with PBS, digested for 15 min with RNase A (50 μg/mL) at 37°C, and stained with propidium iodide (50 μg/mL). The cell DNA contents (10,000 cells per experimental group) were determined with a flow cytometer (FACSCaliber, Becton Dickinson Biosciences) equipped with a ModFit LT program (Verity Software House, Inc.). AGS cells were left untreated or treated for 48 h with two different concentrations of AZD6244 and gefitinib (0.05 and 0.5 μmol/L of AZD6244 and 0.5 and 5 μmol/L of gefitinib), at which point the cells were collected and stained with Annexin V-Fluorescein IsoThioCynate (V–FITC). Apoptotic cell death was assessed by counting the numbers of cells that stained positive for Annexin V–FITC and negative for propidium iodide using an Apoptosis Detection Kit [2] (BD Pharmingen), coupled with fluorescence-activated cell sorting analysis.

Short Interfering RNA Knockdown

Short interfering RNA against HER3 was purchased from Qiagen. Cells were transfected with short interfering RNAs at a final concentration of 40 nmol/L using Lipofectamine 2000 (Invitrogen) in accordance with the manufacturer's instructions. Cell lysates were harvested 48 h after transfection.

In vivo Studies

Animal experiments were conducted in the animal facility of the Seoul National University in accordance with the established institutional guidelines. Six-to-eight-week-old female BALB/c athymic nude mice were purchased from Central Lab Animal, Inc. The mice were permitted to acclimatize to local conditions for 1 wk before being injected with the cancer cells. Thirty mice were injected s.c. into the right flank with AGS cells (1×10^7). When the mice had developed a tumor volume of 50 mm^3, they were randomized into treatment groups ($n = 7$ per group) to receive vehicle (10% ethanol/10% cremophor EL/80% dextrose 5% in water), AZD6244 (24 mg/kg, oral, bd), gefitinib (75 mg/kg, oral, bd), or combination [AZD6244 (25 mg/kg) + gefitinib (75 mg/kg)] treatments, and the experimental drug administration protocol was initiated (day 1). The tumors were then measured with calipers three times per week, and the tumor volume in cubic millimeters was calculated in accordance with the following formula: [(width)^2 × (height)]/2. After the final treatment on day 22, all mice were euthanized.

Terminal Deoxynucleotidyl Transferase–Mediated dUTP Nick End Labeling Assay. Three core tissue biopsies (4 mm in diameter) were obtained from each individual paraffin-embedded tissue sample (donor blocks) and arranged in a new recipient paraffin block (tissue array block) using a trephine apparatus. Each tissue array block contained samples from all animals. Sections of 4 μm were cut from each of the triplicate tissue array blocks, deparaffinized, and dehydrated. Immunohistochemical detection of apoptosis was conducted using an Apoptag *In situ* Apoptosis Detection Kit (Chemicon International), in accordance with manufacturer's recommendations.

Statistical Analysis. An unpaired two-tailed *t* test was used to determine the significance of change in the levels of cell viability and apoptosis between the different treatment groups. Statistical analysis was conducted through *t* tests to compare tumor sizes in the xenograft-bearing mice. Wilcoxon test was used to determine the significance of change in the expression levels of phospho-AKT and -ERK between AZD6244-resistant and -sensitive groups. Differences between groups were considered statistically significant when $P < 0.05$.
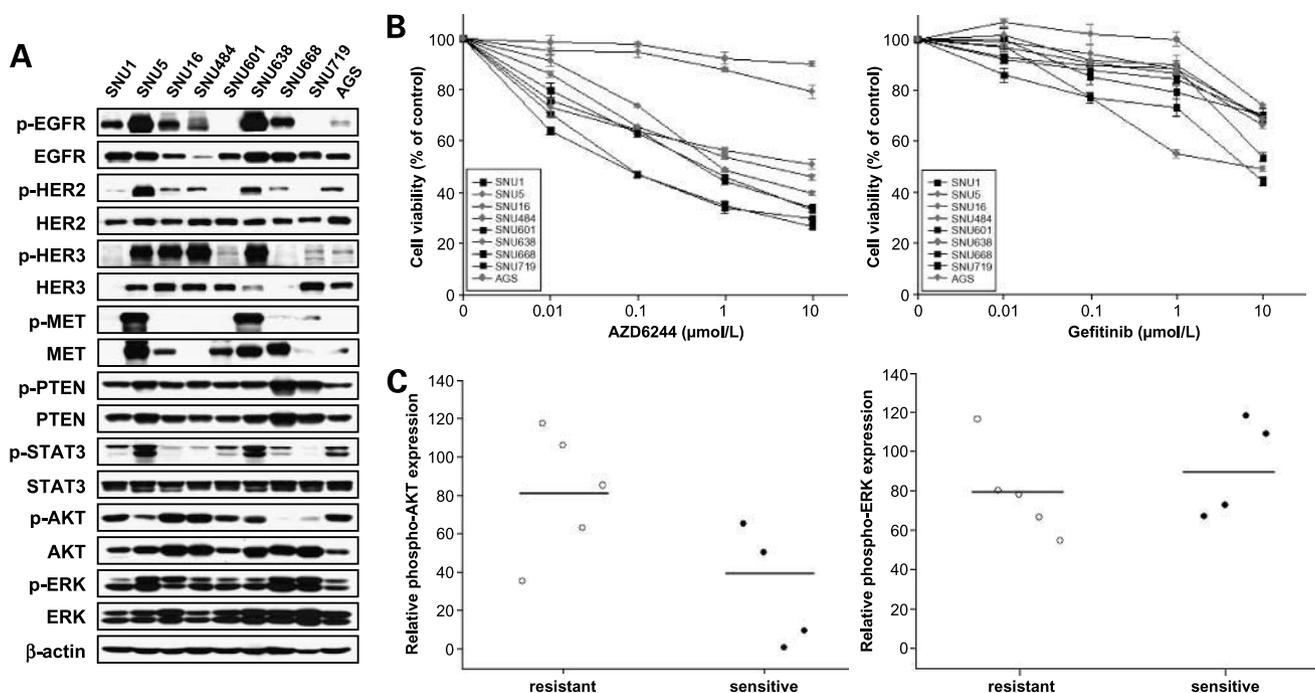
Figure 1. KRAS mutation and/or the basal level of pAKT expression is correlated with AZD6244 sensitivity. **A,** a panel of nine human gastric cancer cells was harvested 24 h after plating and immunoblotted with the indicated antibodies. **B,** the panel of nine human gastric cancer cells was treated with increasing concentrations of gefitinib and AZD6244 (0, 0.01, 0.1, and 10 μmol/L) for 72 h, and cell viability using MTT was determined by measuring the absorbance at 540 nm in a microplate reader. *Bars*, ±SE. Means were derived from six replicates to inhibit the growth of control cells by 50%. **C,** the panel of nine human gastric cancer cells were analyzed by immunoblot for pAKT, total AKT, pERK, and total ERK protein expression. Band intensity was quantified using ImageJ freeware. Cells were grouped as either sensitive (IC$_{50}$, ≤400 nmol/L) or resistant (IC$_{50}$, >400 nmol/L) to the MEK inhibitor AZD6244. Relative pAKT and pERK are shown for the two groups. Only the difference in pAKT between the groups was statistically significant ($P = 0.031$, Wilcoxon test).

Table 1. Sensitivity of gastric cancer cell lines to AZD6244 and gefitinib

Cell lines	KRAS	Others	Gefitinib IC$_{50}$(μmol/L)	AZD6244 IC$_{50}$ (μmol/L)
SNU1	MT, G12D		>10	0.262 ± 0.011
SNU601	MT, G12D		>10	0.068 ± 0.020
SNU668	MT, Q61K		>10	0.034 ± 0.002
AGS	MT, G12D	*PIKCA*, E453K*	>10	0.992 ± 0.043
SNU484	WT		>10	1.370 ± 0.110
SNU719	WT		>10	0.141 ± 0.001
SNU5	WT	*MET* amplification	>10	8.178 ± 1.056
SNU638	WT	*MET* amplification	>10	3.277 ± 0.092
SNU16	WT	*FGFR2* amplification	>10	>10

NOTE: Shown are the IC$_{50}$ values of each drug using MTT assay, as described in the Methods on gastric cancer cell lines.
Abbreviation: MT, mutant.
PIK3CA mutation status is referred to the Wellcome Trust Sanger Institute.

Results

Sensitivity to AZD6244 Is Highly Correlated with KRAS Mutation and/or the Level of pAKT Expression in EGFR WT Gastric Cancer Cells

All of the tested gastric cancer cell lines expressed EGFR (Fig. 1A), and all cell lines were characterized as *EGFR*, *BRAF*, and *PTEN* WTs (data not shown; ref. 30). Four of the nine established gastric cancer cell lines (SNU-1, SNU-601, SNU-668, and AGS) were *KRAS* mutants (Table 1). Interestingly, we noted that genetic alterations of the oncogenes *KRAS* and *PIK3CA* also co-occurred in the AGS cell line. Five of the nine cell lines were identified as *KRAS* WTs; however, SNU-5 and -638 evidenced *MET* gene amplification (16), and SNU16 exhibited *FGFR2* gene amplification (31).

After the characterization of genetic status for each cell line, we conducted growth inhibition assays (Fig. 1B; Table 1). All of the cell lines were resistant to gefitinib (Half Maximal Inhibitory Concentration, >10 μmol/L); however, AZD6244 inhibited the proliferation of some cell lines, and the IC$_{50}$s varied widely, between 0.034 μmol/L and >10 μmol/L. The *KRAS* mutant cell lines, which included SNU-1, SNU-601, and SNU-668, evidenced IC$_{50}$s of AZD6244 of <0.5 μmol/L (range, 0.034–0.262 μmol/L), whereas the AGS cell line with *KRAS* and *PIK3CA* mutations had an IC$_{50}$ of 0.992 μmol/L, relatively higher than those observed in the cell lines harboring the *KRAS* mutation only. Interestingly, the SNU-719 cell line with *KRAS* WT alleles was highly sensitive to AZD6244 (IC$_{50}$, 0.141 μmol/L).

To further characterize sensitivity to MEK inhibition, we conducted conventional quantitation approach (Fig. 1C). As shown in Fig. 1C, AZD6244 sensitivity was independent of the basal expression of pERK. However, there was an inverse correlation between the basal level of pAKT expression and AZD6244 sensitivity ($P = 0.031$).

AZD6244 Induces the G1 Phase Cell Cycle Arrest through the Inhibition of MEK/ERK Pathway but Activates the AKT Pathway in Only AZD6244 Resistant Cancer Cells

In an effort to evaluate the mechanism underlying the effects of AZD6244, we conducted flow cytometric analysis to compare the cell cycle distribution of an AZD6244-sensitive SNU-668 cell line with an AZD6244-resistant SNU-638 cell line (Fig. 2A). Unexpectedly, 24 hours of treatment with increasing doses of AZD6244 (0, 0.05, 0.5, and 5 μmol/L) induced a similar increase in the percentage of cells undergoing G$_1$ phase in the SNU-668 and -638 cell lines. Because the previous studies showed that the RAS/RAF/MEK/ERK pathway regulated the assembly of cyclin D–dependent kinase complexes transcriptionally and posttranslationally, and helped to cancel p27^{kip1}-mediated inhibition (32, 33), we evaluated changes in the expression of cell cycle regulatory molecules, including cyclin D, cyclin E, cyclin A, cyclin B, and p27^{kip1} (Fig. 2B). Cyclin D was down-regulated, but p27^{kip1} was up-regulated in a concentration-dependent manner by AZD6244 in the SNU-668 and -638 cell lines. This indicates that AZD6244 can induce G$_1$ phase cell cycle arrest, regardless of *KRAS* mutation status.

To confirm whether the changes in the expression levels of cell cycle regulating molecules were dependent on the RAS/RAF/MEK/ERK pathway and to further characterize the mechanism of action of AZD6244 in *EGFR* WT gastric cancer cells, we assessed the phosphorylation states of ERK and AKT after 48 hours of treatment with increasing doses of AZD6244 (0, 0.05, 0.5, 5 μmol/L; Fig. 2C). As we had anticipated, ERK phosphorylation was inhibited in the presence of AZD6244 in a concentration-dependent manner in the SNU-668, SNU-719, AGS, and SNU-638 cell lines, regardless of *KRAS* mutation status. By way of contrast, AKT phosphorylation was induced in a concentration-dependent manner in response to MEK inhibition in the AZD6244 resistant cell lines, including the AGS and SNU-638 cell lines, but was inhibited by AZD6244 in the AZD6244-sensitive cell lines such as the SNU-668 and 719 cell lines. These results indicate that the G1 phase cell cycle arrest was induced by AZD6244 through the inhibition of the ERK pathway. However, AKT activation in response to MEK inhibition may prove to be more important in determining the mechanism underlying the effects of AZD6244 in *EGFR* WT gastric cancer cells.

Gefitinib and AZD6244 Show a Synergistic Interaction in *EGFR* WT Gastric Cancer Cells

Treatment with a fixed dose of 0.1 µmol/L of AZD6244, which is below the reported plasma concentrations achievable in humans (34), resulted in a marked enhancement of the antiproliferative effects of gefitinib (Table S1). In cell lines harboring the *KRAS* mutation and *KRAS* and *PI3K* mutations, the IC_{50}s of gefitinib with 0.1 µmol/L of AZD6244 were <0.1 µmol/L (range, 0.008–0.096 µmol/L). In the cell lines containing *KRAS* WT alleles, the IC_{50}s of gefitinib with 0.1 µmol/L of AZD6244 were also relatively reduced as compared with gefitinib alone, but the IC_{50}s varied widely, between 0.01 and 3.18 µmol/L.

In an effort to verify and more accurately characterize the nature of the interaction occurring between gefitinib and AZD6244, multiple drug effect analysis was conducted using a panel of nine gastric cancer cell lines (Fig. 3). The drug concentrations used for these MTT assays ranged between 0.01 and 1 µmol/L for AZD6244 and between 0.1 and 10 µmol/L for gefitinib. *In vitro*, the two agents evidenced profound synergistic interactions against six of nine gastric cancer cell lines with mean index values of 1.28 to 1.54, 1.02 to 1.10, 1.23 to 1.73, 1.60 to 2.04, 1.11 to 1.13, and 1.04 to 1.17 (95% confidence interval; $P < 0.05$) in the *KRAS* mutant SNU-1, -601, and -668, *KRAS* and *PIK3CA* mutant AGS, and *KRAS* WT SNU-484 and -719 cell lines, respectively. These results show that the combination of gefitinib and
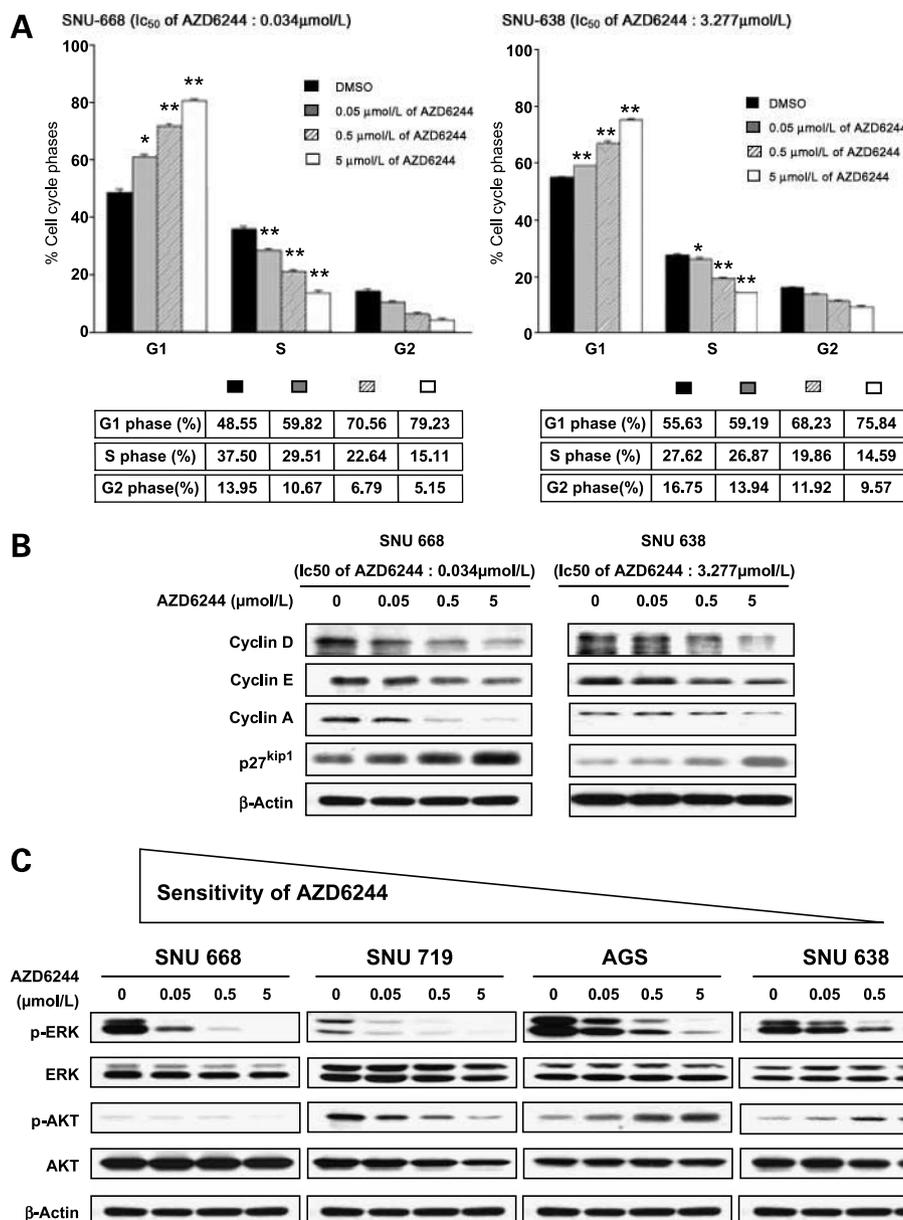
Figure 2. AKT is activated, but ERK is inhibited in response to MEK inhibition. **A,** SNU-668 and -638 cells were treated with the indicated concentrations of AZD6244 for 24 h. Cells were used for flow cytometric analysis of cell cycle distribution. Percentages of cells in G_1, S, and G_2 phases of the cell cycle are shown. *Columns*, mean of three independent experiments; *bars*, ±SE. *, $P < 0.05$; **, $P < 0.01$. **B,** Western blotting was conducted for cyclins D, E, A, B, and $p27^{kip1}$ with SNU-668 and -638 cells after treatment with the indicated concentrations of AZD6244 for 48 h. **C,** SNU-668, SNU-719, AGS, and SNU-638 cells were exposed to the indicated concentrations of AZD6244 for 48 h. The cell lysates were subjected to Western blotting with the indicated antibodies.
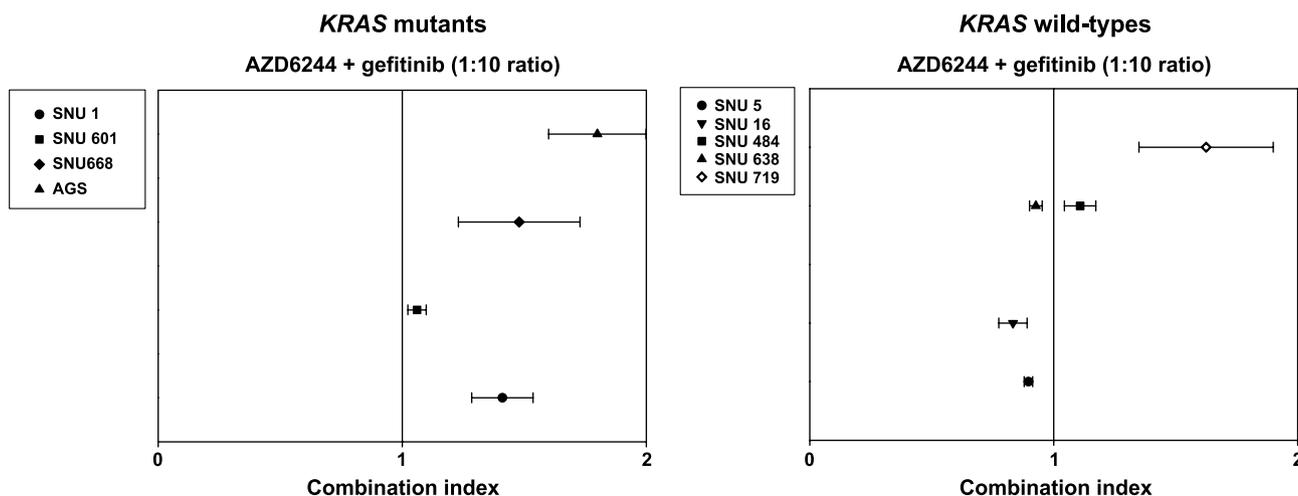
Figure 3. Inhibition of EGFR and MEK synergistically enhances antiproliferative effects in human gastric cancer cell lines. The panel of nine human gastric cancer cells was treated with AZD6244 and gefitinib in a 1:10 ratio, and cell viability using MTT was determined by measuring absorbance at 540 nm in a microplate reader. Index values that are statistically significantly >1 indicate synergistic interactions. Index values that are statistically significantly <1 indicate antagonistic interactions. Index values equal to (or not statistically significantly different from) 1 indicate additive interactions. *Bars*, ±SE. Mean is derived from six replicates to inhibit the growth of control cells by 50%.

AZD6244 synergistically enhanced the antiproliferative effects in subsets of *EGFR* WT gastric cancer cells *in vitro*.

Addition of Gefitinib Inhibits AKT Activation through the Suppression of Activating EGFR/HER3 Signaling Pathways

To determine whether upstream RTKs mediated the aberrant activation of the AKT pathway in response to MEK inhibition, we used phospho-RTK and phospho-MAPK arrays to compare the effects of AZD6244, gefitinib, or AZD6244 in combination with gefitinib on the AGS cell line, in which the two drugs had been shown to exert a synergistic effect on cell proliferation (Fig. 4A). The results of the phospho-RTK and -MAPK arrays showed that EGFR, HER2, HER3, and AKT were all phosphorylated; however, this phosphorylation was markedly elevated in the presence of AZD6244 for 48 hours. By way of contrast, gefitinib treatment induced a significant reduction in that phosphorylation. This observation indicates that a complementary relationship may exist between gefitinib and AZD6244 in the AGS cell line, and this may be attributed to the fact that AZD6244 inhibits the MEK/ERK pathway but somehow induces EGFR/HER3-mediated AKT activation, whereas gefitinib inhibits EGFR/HER3-mediated AKT activation but does not inhibit the MEK/ERK pathway.

In an effort to further confirm whether complementary effects between gefitinib and AZD6244 might be a mechanism underlying the observed synergistic effects, we assessed the phosphorylation state of RTKs and downstream signaling molecules after administering AZD6244, gefitinib, or combined treatment at the indicated doses for 48 hours in the AGS cell line, which showed synergism, and in the SNU-638 cell line, which exhibited antagonism (Fig. 4B). In the AGS cell line, gefitinib and AZD6244 induced a dramatic inhibition of EGFR/HER3-mediated ATK, as well as the MEK/ERK pathway in a concentration-dependent fashion.

By way of contrast, the SNU-638 cell line maintained the activation of MET, HER3, and AKT pathways in the presence of gefitinib and AZD6244. Furthermore, the combined treatment had similar effects in the SNU-484 cell line, which showed synergism, and in the SNU-5 and -16 cell lines, which exhibited antagonism (Supplementary Fig. S1).

To validate a rational basis for choosing which inhibitor to combine with the MEK inhibitor in cells on the basis of the expression and amplification of different RTKs, we conducted a multiple drug effect analysis using SU11274, a MET inhibitor, and AZD6244 in a *MET* gene–amplified SNU638 cell line (Supplementary Fig. S2A). The drug concentrations used for these MTT assays ranged between 0.01 and 1 μmol/L for AZD6244 and between 0.1 and 10 μmol/L for SU11274. *In vitro*, the two agents evidenced profound synergistic interactions with mean index values of 1.01 to 1.08 (95% confidence interval; $P < 0.05$) in the SNU-638 cells. We also conducted an immunoblotting assay to compare the effects of AZD6244 (1 μmol/L), SU11274 (1 μmol/L), or AZD6244 plus SU11274 (1 μmol/L, respectively) on the SNU-638 cell line, which exhibited antagonism with a combination of gefitinib and AZD6244 (Supplementary Fig. S2B). The results showed that the combined treatment of AZD6244 and SU11274 induced a dramatic inhibition of MET-mediated ATK as well as the MEK/ERK pathway in the SNU-638 cells.

Dual Inhibition of EGFR and MEK1/2 Signaling Pathways Enhanced Cell Death and Delayed Tumor Growth

As a single agent, AZD6244 treatment applied to human gastric cancer cell lines resulted in an induction of G_1 phase cell cycle arrest, but not apoptosis. To determine whether complementary interactions of gefitinib with AZD6244 induce apoptosis, we conducted flow cytometric analysis to determine the percentage of sub-G_1 cells, which is consistent

with the induction of apoptosis, in AGS and SNU-638 cell lines (Fig. 5A). In the AGS cell line, treatment with 0.05 or 0.5 μmol/L of AZD6244 for 24 hours yielded a percentage of cells with a sub-G_1 population from 3% to 7% and 8%, respectively. However, the concurrent treatment with gefitinib (0.5–5 μmol/L) and AZD6244 (0.05–0.5 μmol/L) for 24 hours in the AGS cell line resulted in the induction of apoptosis from 3% to 8%, 9%, 11%, and 13%, respectively. In the SNU-638 cell line, the percentage of the sub-G_1 portion remained largely unaltered (data not shown). In an effort to confirm and more accurately evaluate the apoptotic response, the AGS cell line was subjected to an Annexin V–FITC apoptosis assay (Fig. 5A). These data confirmed the induction of robust concentration-dependent apoptosis through a combined treatment of gefitinib with AZD6244 in the AGS cell line. By way of contrast, apoptosis was not detected in the SNU-638 cells (data not shown).

The induced apoptosis observed subsequent to treatment with gefitinib and AZD6244 may be attributable to the abrogation of transactivated HER3-mediated AKT activation and the MEK/ERK pathway; however, tyrosine kinase inhibitors frequently have off-target effects (35). In an effort to assess the induced apoptosis results from inhibition of HER3 activity by gefitinib and MEK activity
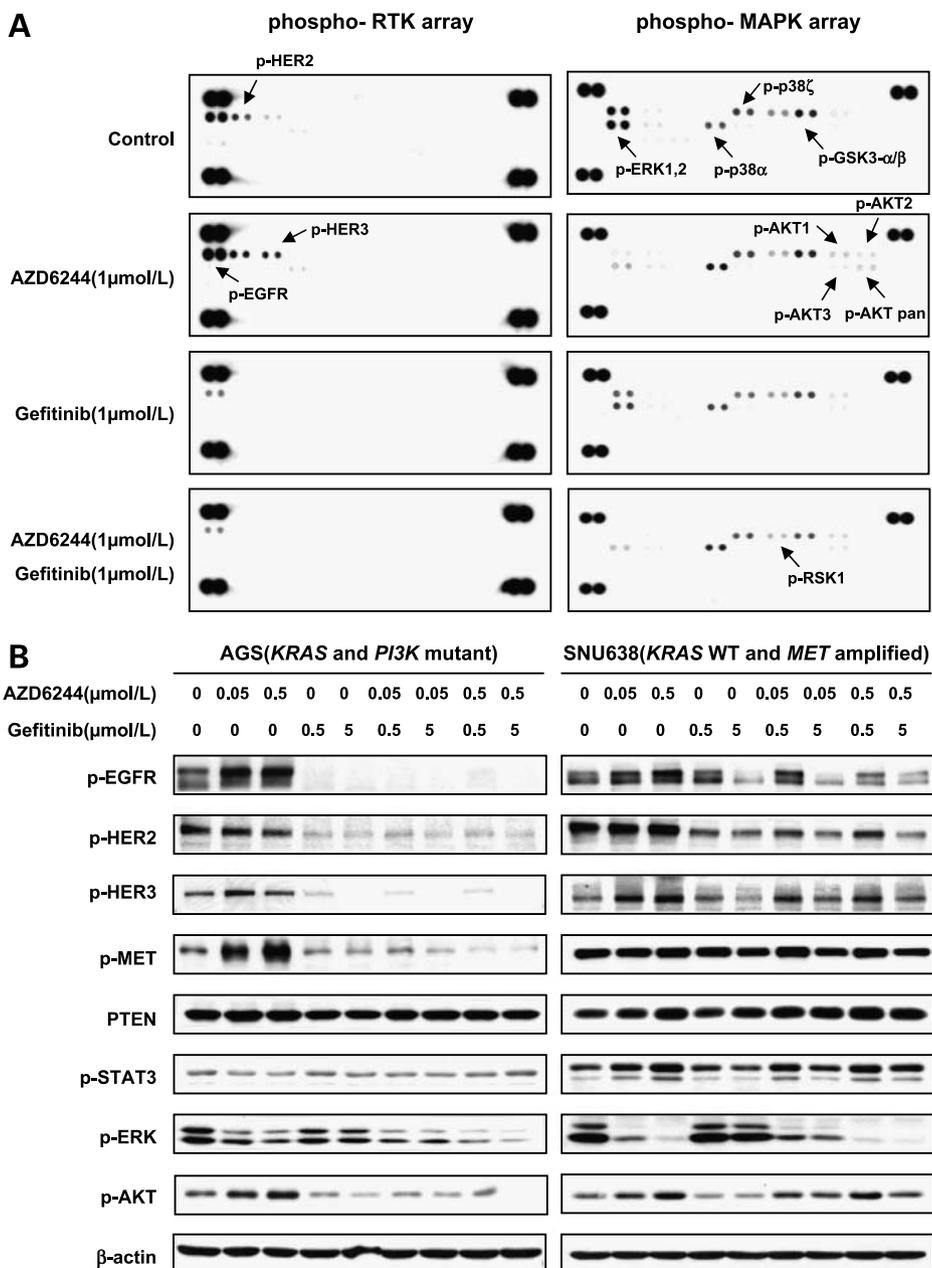
Figure 4. AKT activation in response to MEK inhibition is inhibited by gefitinib through suppressing EGFR/HER3 signaling pathway. **A,** AGS cells were treated with AZD6244, gefitinib, or AZD6244 plus gefitinib at the indicated concentrations for 48 h, and the cell lysates were hybridized to phospho-RTK and -MAPK arrays. In the arrays, each RTK and MAPK is spotted in duplicate. Hybridization signals at the corners serve as controls. **B,** AGS and SNU-638 cells were treated with AZD6244, gefitinib, or AZD6244 plus gefitinib at the indicated concentrations for 48 h. The cell lysates were immunoblotted with the indicated antibodies.

Figure 5. Combination of gefitinib and AZD6244 induces enhanced apoptosis through suppressing PI3K/AKT signaling pathway. **A,** AGS and SNU-638 cells were treated with the indicated concentrations of AZD6244, gefitinib, or AZD6244 plus gefitinib for 24 h. Cells were used for flow cytometric analysis of cell cycle distribution and Annexin V apoptosis assays, as described in the Methods section. *Columns,* mean of three independent experiments; *bars,* ±SE. *, $P < 0.05$; **, $P < 0.01$. **B,** AGS cells were transfected with control and HER3 short interfering RNAs. After 24 h, the cells were changed to fresh culture medium and treated with DMSO or AZD6244 (1 μmol/L). AGS cells were harvested for cell cycle assays or apoptosis at 48 h after treatment. *Columns,* mean of three independent experiments; *bars,* ±SE. *, $P < 0.05$; **, $P < 0.01$. **C,** AGS cells were treated with the indicated concentrations of AZD6244, LY294002, or AZD6244 plus LY294002 for 24 h. Cells were used for flow cytometric analysis of cell cycle distribution and Annexin V apoptosis assays, as described in the Methods section. *Columns,* mean of three independent experiments; *bars,* ±SE. *, $P < 0.05$; **, $P < 0.01$. **D,** AGS cells were treated with the indicated concentrations of AZD6244, gefitinib, or AZD6244 plus gefitinib for 48 h. AGS cells were also treated with the indicated concentrations of AZD6244, LY294002, or AZD6244 plus LY294002 for 48 h. Cell lysates were immunoblotted with indicated antibodies.
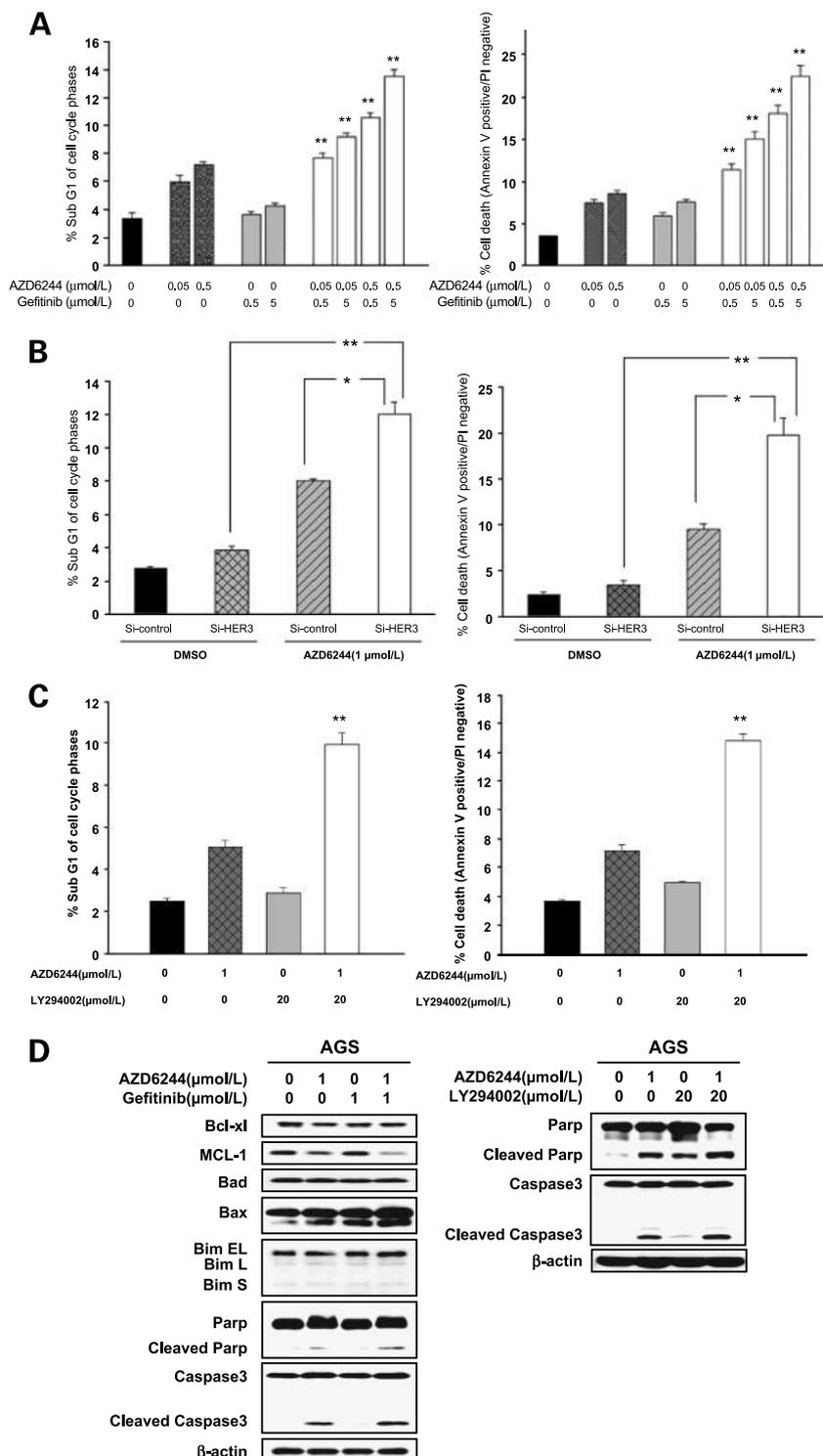
by AZD6244, HER3 function was directly inhibited by using short interfering RNA to down-regulate HER3 protein expression with MEK inhibition in the AGS cell line (Supplementary Fig. S3). To evaluate the apoptotic effects of HER3 knockdown with MEK inhibition, we conducted flow cytometric analysis using propidium iodide (13) and Annexin V–FITC (Fig. 5B). The percentage of sub-G$_1$ and Annexin V–positive/propidium iodide-negative cells was increased significantly after the knockdown of HER3 proteins and MEK inhibition as compared with the knockdown of HER3 proteins or MEK inhibition only in the AGS cell line.

Because the key mechanism of the synergistic interaction between AZD6244 and gefitinib seems to be the blockade of activated PI3K/AKT pathway in response to AZD6244 treatment, we used LY294002, a PI3K inhibitor with AZD6244 to verify whether the potentially synergistic effects of gefitinib are mediated through PI3K (Fig. 5C and D). The results from flow cytometric analysis using propidium iodide (13) and Annexin V–FITC showed that the activation of PI3K/AKT pathway in response to MEK inhibition played a role in the observed synergy of the MEK and EGFR inhibitor combination.

Next, we assessed the expression levels of apoptosis-regulating molecules in the AGS cell line (Fig. 5D). The levels of the antiapoptotic protein MCL-1 and the proapoptotic protein BAX were significantly altered, and poly(ADP-ribose) polymerase and caspase-3 cleavage were increased after 48 hours of combined treatment of AZD6244/gefitinib and AZD6244/LY294002. Interestingly, the proapoptotic BH3-only protein BIM was not significantly induced by treatment with the combination of gefitinib and AZD6244. Although the mechanism underlying apoptosis in oncogenic EGFR mutants has been previously studied (36–38), the mechanism underlying apoptosis in *EGFR* WTs remains to be clearly elucidated.

The synergistic proapoptotic effects of EGFR and MEK inhibition imply that the targeting of EGFR and MEK signaling may constitute a rational strategy for the treatment of *EGFR* WT gastric tumors. Therefore, we attempted to determine whether the inhibition of both pathways *in vivo* would effectively suppress tumor growth in a human AGS xenograft model (Fig. 6). The volumes in mice receiving daily coadministration of AZD6244 (25 mg/kg) and gefitinib (75 mg/kg) was significantly smaller than that observed in the vehicle control, AZD6244, and gefitinib alone groups ($P < 0.001$; $P < 0.05$; $P < 0.05$). The effects of the combination treatment on apoptosis were also assessed using an AGS xenograft model (Fig. 6). We conducted a terminal deoxynucleotidyl transferase–mediated dUTP nick end labeling assay on paraffin-embedded xenograft tumors and used tissue arrays, which allowed for a direct comparison between tissues from different animal groups. The levels of apoptotic positive cells detected in the AZD6244 and gefitinib coadministration groups were higher than those detected in the other groups.
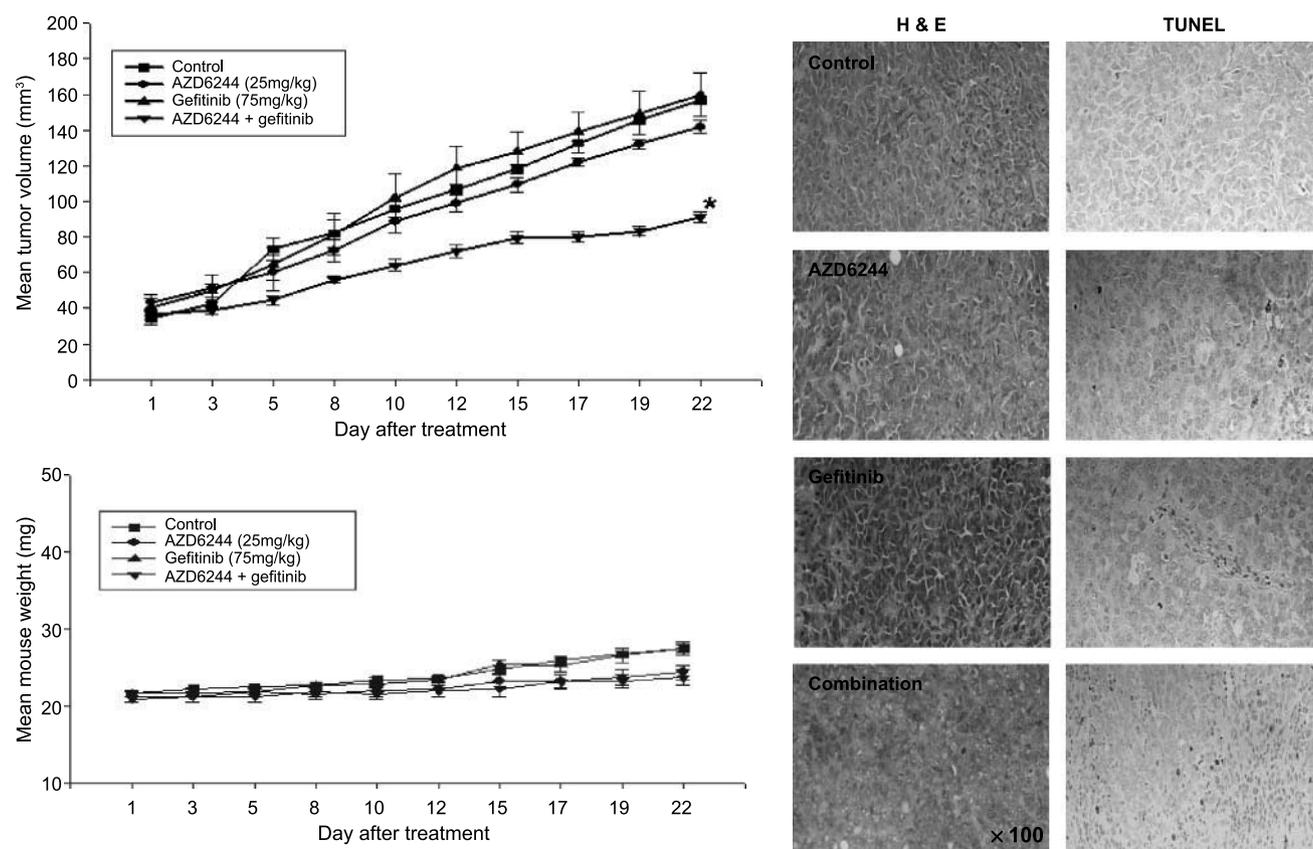
Figure 6. Combination of gefitinib and AZD6244 significantly delayed tumor growth in a human AGS xenograft model. AGS cells were grown as tumor xenografts in nude mice. After tumor establishment (50 mm^3), mice were treated p.o. for 21 d daily with AZD6244 (25 mg/kg), gefitinib (75 mg/kg), or AZD6244 (25 mg/kg) plus gefitinib (75 mg/kg). Tumors were measured thrice per week using calipers. *, $P < 0.05$ at day 21. Terminal deoxynucleotidyl transferase–mediated dUTP nick end labeling assay was conducted with the control, AZD6244, gefitinib, or AZD6244 plus gefitinib groups. Apoptosis was measured in paraffin-embedded xenograft tumors, and representative images of terminal deoxynucleotidyl transferase–mediated dUTP nick end labeling immohistochemistry are shown.

These results reinforce the notion that the complementary inhibition of EGFR and MEK signaling pathways by gefitinib and AZD6244 induced synergistic growth inhibition *in vivo* as well as *in vitro*, and thus, the targeted dual inhibition of EGFR and MEK may constitute a rational therapeutic strategy for the treatment of subsets of *EGFR* WT gastric cancers.

Discussion

Tumor cells seem to depend strongly on the constitutive activation of one or two pathways, a phenomenon which has been termed oncogene addiction, whereas normal cells utilize a broader range of pathways (3). This oncogene addiction may constitute an "Achilles' heel" within the cancer cells, which can be exploited therapeutically by targeting the pathways activated by oncogenes such as *EGFR* (4, 5, 19, 39). Moreover, other oncogene mutations that activate common downstream pathways, such as AKT and ERK, can co-occur, such as in the case of *PI3K* with *EGFR* or *KRAS* in human cancers (20). Multiple cancer genes may also simultaneously interact in human cancers, and these phenomena present a significant challenge to the development of more potent and rational molecular targeted therapeutic strategies.

Activating mutations in *EGFR* or *KRAS* have been well characterized in human cancers. The activation of each oncogene by mutation and/or amplification subsequently activates downstream AKT and/or ERK signals for survival. Mutations in the *EGFR* gene are detected only in a minority of non–small cell lung cancers, and these mutations are correlated strongly with responses to tyrosine kinase inhibitors (7–12). However, tyrosine kinase inhibitors have limited activity in most tumors with *EGFR* WT alleles. The molecular mechanisms of tyrosine kinase inhibitors resistance in *EGFR* WT tumors remain poorly understood. A previous study showed that gefitinib completely suppressed EGFR phosphorylation, but ERK phosphorylation was increased by the administration of gefitinib treatment in *EGFR* WT cancer cells (18); additionally, it has been suggested that the role of ERK activation might be that of a resistance mechanism. By way of contrast with the relatively uncommon *EGFR* mutations, *KRAS* mutations are common in human cancers and are frequently detected in subsets of *EGFR* WT tumors (17, 18). *KRAS* mutations have been shown to induce primary resistance to EGFR inhibitors owing to the persistent activation of RAS/MAPK pathways (15, 21). The results of a recent study have shown that AZD6244, a novel MEK inhibitor, is active in preclinical tumor models containing *KRAS* or *BRAF* mutations (40). However, another study has shown that U0126, a MEK inhibitor, induces the association of Gab1 and PI3K with EGFR and results in increased AKT phosphorylation in U0126-resistant cells (41). Accordingly, it seems that either ERK or AKT is activated as a counterpart signal when cells are exposed to EGFR or MEK inhibitors. Thus, we hypothesized that the dual inhibition of EGFR and MEK signaling pathways would result in enhanced antiproliferative and antitumor effects in *EGFR* WT gastric tumors.

Via a growth inhibition assay, we determined that gefitinib was ineffective in all gastric cancer cell lines; however, AZD6244 was effective in four cell lines (three *KRAS* mutant and one *KRAS* WT). The high degree of sensitivity of SNU-719 cell lines, characterized as *EGFR, KRAS, BRAF,* and *PI3K* WTs, to AZD6244 treatment was unexpected, considering its genetic status. Moreover, PTEN is basally expressed in the SNU-719 cell line (Fig. 1A). The results of a recent study showed that MEK dependence was correlated inversely with the level of pAKT basal expression (42). In the SNU-719 cell line, the basal expression of pAKT was relatively lower than in other cell lines (Fig. 1C). These basal pAKT levels may explain, at least in part, why AZD6244 is sensitive to the SNU-719 cell line. Furthermore, this finding shows that the basal pAKT level as well as the *KRAS* mutation status should be considered in the treatment of gastric cancers with AZD6244.

Additionally, our results indicated that the inhibition of EGFR and MEK synergistically enhanced apoptosis *in vitro* and/or *in vivo* in *EGFR* WT gastric cancer cell lines. EGFR-mediated AKT activation and MEK-mediated ERK activation are significantly inhibited as the consequence of a complementary interaction that occurs between AZD6244 and gefitinib in six out of nine gastric cancer cell lines. However, the remaining three cell lines exhibiting either additional MET amplification or FGFR amplification did not respond to combination treatment. This is understandable because the results of a recent study have shown that EGFR or MET can transactivate other receptor tyrosine kinases, according to the dependency of EGFR and MET (43). Constitutive MET activation may transactivate HER3/AKT signaling pathways in the SNU-638 cell line, unlike the EGFR/HER3-mediated AKT activation observed in the AGS cell line, because the combination of AZD6244 and SU11274 exerts a synergistic effect and inhibits the phosphorylation of AKT and ERK. These results provide a rational basis for choosing which inhibitor to combine with a MEK inhibitor in cells on the basis of the expression and amplification of different RTKs.

Finally, a synergistic interaction between gefitinib and AZD6244 was noted in the AGS xenograft model. However, this combination resulted in delayed tumor growth, but not tumor regression. This may be attributable to the selected doses of AZD6244 (25 mg/kg) and gefitinib (75 mg/kg). In a previous study, the activity of AZD6244 in *in vivo* xenograft models was tested at various doses (10, 25, 50, 100 mg/kg; ref. 44). Based on the results of this study, 25 mg/kg of AZD6244 may be a low dose, but no clinical signs of toxicity were noted in mice receiving 25 mg/kg of AZD6244 and 75 mg/kg of gefitinib (Fig. 6). Therefore, this *in vivo* study should be expanded, and future studies should be attempted to ascertain whether the results presented herein translate into clinical therapeutic efficacy.

In this study, we have shown a complementary activity between gefitinib and AZD6244 against subsets of *EGFR* WT gastric cancer cells in *in vitro* and *in vivo* contexts. These findings provide a clear biological rationale for the testing of AZD6244 in combination with gefitinib in *EGFR* WT gastric cancers.

Disclosure of Potential Conflicts of Interest

No potential conflicts of interest were disclosed.

References

1. Downward J. Cancer biology: signatures guide drug choice. Nature 2006;439:274–5.

2. Krause DS, Van Etten RA. Tyrosine kinases as targets for cancer therapy. N Engl J Med 2005;353:172–87.

3. Weinstein IB. Cancer. Addiction to oncogenes—the Achilles heal of cancer. Science 2002;297:63–4.

4. Weinstein IB, Joe AK. Mechanisms of disease: oncogene addiction—a rationale for molecular targeting in cancer therapy. Nat Clin Pract Oncol 2006;3:448–57.

5. Sharma SV, Settleman J. Oncogene addiction: setting the stage for molecularly targeted cancer therapy. Genes Dev 2007;21:3214–31.

6. Gschwind A, Fischer OM, Ullrich A. The discovery of receptor tyrosine kinases: targets for cancer therapy. Nat Rev Cancer 2004;4:361–70.

7. Paez JG, Janne PA, Lee JC, et al. EGFR mutations in lung cancer: correlation with clinical response to gefitinib therapy. Science 2004;304: 1497–500.

8. Lynch TJ, Bell DW, Sordella R, et al. Activating mutations in the epidermal growth factor receptor underlying responsiveness of non-small-cell lung cancer to gefitinib. N Engl J Med 2004;350:2129–39.

9. Pao W, Miller V, Zakowski M, et al. EGF receptor gene mutations are common in lung cancers from "never smokers" and are associated with sensitivity of tumors to gefitinib and erlotinib. Proc Natl Acad Sci U S A 2004;101:13306–11.

10. Han SW, Kim TY, Hwang PG, et al. Predictive and prognostic impact of epidermal growth factor receptor mutation in non-small-cell lung cancer patients treated with gefitinib. J Clin Oncol 2005;23:2493–501.

11. Kobayashi S, Boggon TJ, Dayaram T, et al. EGFR mutation and resistance of non-small-cell lung cancer to gefitinib. N Engl J Med 2005;352: 786–92.

12. Pao W, Miller VA, Politi KA, et al. Acquired resistance of lung adenocarcinomas to gefitinib or erlotinib is associated with a second mutation in the EGFR kinase domain. PLoS Med 2005;2:e73.

13. Stephens P, Hunter C, Bignell G, et al. Lung cancer: intragenic ERBB2 kinase mutations in tumours. Nature 2004;431:525–6.

14. Samuels Y, Wang Z, Bardelli A, et al. High frequency of mutations of the *PIK3CA* gene in human cancers. Science 2004;304:554.

15. Pao W, Wang TY, Riely GJ, et al. KRAS mutations and primary resistance of lung adenocarcinomas to gefitinib or erlotinib. PLoS Med 2005;2:e17.

16. Smolen GA, Sordella R, Muir B, et al. Amplification of MET may identify a subset of cancers with extreme sensitivity to the selective tyrosine kinase inhibitor PHA-665752. Proc Natl Acad Sci U S A 2006; 103:2316–21.

17. Downward J. Targeting RAS signalling pathways in cancer therapy. Nat Rev Cancer 2003;3:11–22.

18. Friday BB, Adjei AA. K-ras as a target for cancer therapy. Biochim Biophys Acta 2005;1756:127–44.

19. Gazdar AF, Shigematsu H, Herz J, Minna JD. Mutations and addiction to EGFR: the Achilles 'heal' of lung cancers? Trends Mol Med 2004;10: 481–6.

20. Thomas RK, Baker AC, Debiasi RM, et al. High-throughput oncogene mutation profiling in human cancer. Nat Genet 2007;39:347–51.

21. de Reynies A, Boige V, Milano G, Faivre J, Laurent-Puig P. KRAS mutation signature in colorectal tumors significantly overlaps with the cetuximab response signature. J Clin Oncol 2008;26:2228–30; author reply 30-1.

22. Jimeno A, Rubio-Viqueira B, Amador ML, et al. Dual mitogen-activated protein kinase and epidermal growth factor receptor inhibition in biliary and pancreatic cancer. Mol Cancer Ther 2007;6:1079–88.

23. Lev DC, Kim LS, Melnikova V, et al. Dual blockade of EGFR and ERK1/2 phosphorylation potentiates growth inhibition of breast cancer cells. Br J Cancer 2004;91:795–802.

24. Mirzoeva OK, Das D, Heiser LM, et al. Basal subtype and MAPK/ERK kinase (MEK)-phosphoinositide 3-kinase feedback signaling determine susceptibility of breast cancer cells to MEK inhibition. Cancer Res 2009; 69:565–72.

25. Singer G, Oldt R III, Cohen Y, et al. Mutations in BRAF and KRAS characterize the development of low-grade ovarian serous carcinoma. J Natl Cancer Inst 2003;95:484–6.

26. Edkins S, O'Meara S, Parker A, et al. Recurrent KRAS codon 146 mutations in human colorectal cancer. Cancer Biol Ther 2006;5:928–32.

27. Ku JL, Park JG. Biology of SNU cell lines. Cancer Res Treat 2005;37: 1–19.

28. Kim HP, Han SW, Kim SH, et al. Combined lapatinib and cetuximab enhance cytotoxicity against gefitinib-resistant lung cancer cells. Mol Cancer Ther 2008;7:607–15.

29. Morgillo F, Kim WY, Kim ES, et al. Implication of the insulin-like growth factor-IR pathway in the resistance of non-small cell lung cancer cells to treatment with gefitinib. Clin Cancer Res 2007;13:2795–803.

30. Park JG. SNU cell lines and their application for cancer research. Gan To Kagaku Ryoho 2002;29 Suppl 1:89–98.

31. Kunii K, Davis L, Gorenstein J, et al. FGFR2-amplified gastric cancer cell lines require FGFR2 and Erbb3 signaling for growth and survival. Cancer Res 2008;68:2340–8.

32. Peeper DS, Upton TM, Ladha MH, et al. Ras signalling linked to the cell-cycle machinery by the retinoblastoma protein. Nature 1997;386: 177–81.

33. Cheng M, Sexl V, Sherr CJ, Roussel MF. Assembly of cyclin D-dependent kinase and titration of p27Kip1 regulated by mitogen-activated protein kinase (MEK1). Proc Natl Acad Sci U S A 1998;95:1091–6.

34. Adjei AA, Cohen RB, Franklin W, et al. Phase I pharmacokinetic and pharmacodynamic study of the oral, small-molecule mitogen-activated protein kinase kinase 1/2 inhibitor AZD6244 (ARRY-142886) in patients with advanced cancers. J Clin Oncol 2008;26:2139–46.

35. Karaman MW, Herrgard S, Treiber DK, et al. A quantitative analysis of kinase inhibitor selectivity. Nat Biotechnol 2008;26:127–32.

36. Cragg MS, Kuroda J, Puthalakath H, Huang DC, Strasser A. Gefitinib-induced killing of NSCLC cell lines expressing mutant EGFR requires BIM and can be enhanced by BH3 mimetics. PLoS Med 2007;4:1681–89; discussion 90.

37. Costa DB, Halmos B, Kumar A, et al. BIM mediates EGFR tyrosine kinase inhibitor-induced apoptosis in lung cancers with oncogenic EGFR mutations. PLoS Med 2007;4:1669–79; discussion 80.

38. Gong Y, Somwar R, Politi K, et al. Induction of BIM is essential for apoptosis triggered by EGFR kinase inhibitors in mutant EGFR-dependent lung adenocarcinomas. PLoS Med 2007;4:e294.

39. Mellinghoff I. Why do cancer cells become "addicted" to oncogenic epidermal growth factor receptor? PLoS Med 2007;4:1620–2.

40. Friday BB, Yu C, Dy GK, et al. BRAF V600E disrupts AZD6244-induced abrogation of negative feedback pathways between extracellular signal-regulated kinase and Raf proteins. Cancer Res 2008;68: 6145–53.

41. Yu CF, Liu ZX, Cantley LG. ERK negatively regulates the epidermal growth factor-mediated interaction of Gab1 and the phosphatidylinositol 3-kinase. J Biol Chem 2002;277:19382–8.

42. Pratilas CA, Hanrahan AJ, Halilovic E, et al. Genetic predictors of MEK dependence in non-small cell lung cancer. Cancer Res 2008;68: 9375–83.

43. Guo A, Villen J, Kornhauser J, et al. Signaling networks assembled by oncogenic EGFR and c-Met. Proc Natl Acad Sci U S A 2008;105: 692–7.

44. Yeh TC, Marsh V, Bernat BA, et al. Biological characterization of ARRY-142886 (AZD6244), a potent, highly selective mitogen-activated protein kinase kinase 1/2 inhibitor. Clin Cancer Res 2007;13:1576–83.

AAC R American Association
for Cancer Research

Molecular Cancer Therapeutics

Combination of EGFR and MEK1/2 inhibitor shows synergistic effects by suppressing EGFR/HER3-dependent AKT activation in human gastric cancer cells

Young-Kwang Yoon, Hwang-Phill Kim, Sae-Won Han, et al.

Updated version	Access the most recent version of this article at: doi:10.1158/1535-7163.MCT-09-0300
Supplementary Material	Access the most recent supplemental material at: http://mct.aacrjournals.org/content/suppl/2009/09/16/1535-7163.MCT-09-0300.DC1

Cited articles	This article cites 44 articles, 20 of which you can access for free at: http://mct.aacrjournals.org/content/8/9/2526.full#ref-list-1
Citing articles	This article has been cited by 13 HighWire-hosted articles. Access the articles at: http://mct.aacrjournals.org/content/8/9/2526.full#related-urls

E-mail alerts	Sign up to receive free email-alerts related to this article or journal.
Reprints and Subscriptions	To order reprints of this article or to subscribe to the journal, contact the AACR Publications Department at pubs@aacr.org.
Permissions	To request permission to re-use all or part of this article, use this link http://mct.aacrjournals.org/content/8/9/2526. Click on "Request Permissions" which will take you to the Copyright Clearance Center's (CCC) Rightslink site.